Defining and phenotyping gastric abnormalities in long-term type 1 diabetes using body surface gastric mapping

Phenotyping gastric abnormalities in type 1 diabetes

Authors: William Xu[1], Armen A. Gharibans[1,2,3], Stefan Calder[1,2], Gabriel Schamberg[1,2], Anthony Walters[4], Jia Jang[1], Chris Varghese[1], Daniel Carson[1], Charlotte Daker[2], Stephen Waite[2], Christopher N Andrews[2,5], Tim Cundy[6], Gregory O'Grady[1,2,3]

Affiliations

1. Department of Surgery, the University of Auckland, New Zealand
2. Alimetry Ltd, Auckland, New Zealand
3. Auckland Bioengineering Institute, The University of Auckland, New Zealand
4. Liggins Institute, University of Auckland, New Zealand
5. Dept of Gastroenterology, University of Calgary, Canada
6. Department of Medicine, University of Auckland, New Zealand

Supplementary materials

Contents

Supplementary methods

Assessment of diabetes complications

Retinopathy

Retinopathy was diagnosed based on ophthalmology clinical reports and classified as either no disease, mild to moderate diabetic retinopathy, or severe disease (severe non-proliferative or pre-proliferative diabetic retinopathy or proliferative retinopathy).

Nephropathy and neuropathy

Nephropathy was graded based on estimated glomerular filtration rate (eGFR) thresholds and clinical records (1). A diagnosis of peripheral neuropathy was made based on clinical electronic records as documented by endocrinology or neurology consult notes.

Cardiovascular and autonomic dysfunction

Patients had a diagnosis of hypertension and ischemic heart disease recorded from clinical records. Orthostatic hypotension was assessed as a screening tool for sympathetic nervous system dysfunction and was defined as >20mmHg drop in systolic blood pressure or >10mmg drop in diastolic after 5 minutes supine and 1 minute of upright standing (2).

Gastric Alimetry® System

Section adapted from Gharibans et al. (3)

Gastric Alimetry® is a novel medical device custom designed for BSGM. The device consists of an HR Array, wearable Reader, Dock, iPadOS App for setup and symptom logging, and cloud-based analytics and reporting platform **(Fig. S1A**). Key design considerations for each component are detailed below.

- Array. The Gastric Alimetry Array™ includes 66 pre-gelled Ag/AgCl electrodes (8×8 grid +2 reference; inter-electrode spacing 20 mm), covering an area of 21×16 cm (196 cm2) **(Fig. S1B**). This Array™ specification was designed to overlie the majority of the stomach's area in >95% of cases, which is important because gastric position is highly variable, and the weak gastric signal strength diminishes exponentially from source (4–6). Each Array is single-use, being screen printed using conductive inks on a single, flexible, thermoplastic polyurethane (TPU), with an overlying peel-and-stick adhesive layer that enables rapid setup and removal (7).
- Reader. The Alimetry Reader™ incorporates custom-designed electronics specifically tuned for gastric electrophysiology (**Fig. S1B**). Signals are acquired at 250 Hz, then amplified and digitized by low-noise programmable gain amplifiers, with each input compared against a common reference electrode to provide unipolar recordings, while movement artifacts are registered by an onboard accelerometer. The Reader attaches to the Array using a custom board-to-board connector design that eliminates all cabling to enable unimpeded wearability and facilitate ease of cleaning.
- Dock. The Alimetry Dock™ is used for charging and storage of the Reader, and accurate alignment of the Array during setup (**Fig. S1B**).

- App. The Gastric Alimetry App™ runs on an iPad mini (Apple, Cupertino, CA), and is used for device setup, data transfers, and to capture patient-reported symptom data during testing. Guided setup in the App includes an Array positioning step that tailors placement per individual patient biometrics, to further enhance accurate positioning over the stomach (7). Patients log symptoms every 15 minutes via a digital interface employing pictograms (**Fig. S1A**), which has been validated to enable reliable capture of patient symptom data in association with a standard meal with excellent compliance (8) This system therefore enables precise temporal correlations between patient symptom profiles with electrophysiological data.
- Cloud / Portal. Test data is transmitted to a HIPAA-compliant cloud server at the conclusion of each test. A proprietary algorithm automatically filters and analyzes raw myoelectrical signals to generate a report, including key metrics and data visualizations (detailed below), which are accessible via a secure online portal. Filtering methods are based on a previously validated scheme by Gharibans et al, accounting for accelerometer data (9).

Spatial and spectral data analytics

SPECTRAL ANALYSIS

BSGM spectrograms visualize the bioelectrical slow waves that coordinate gastric activity, as well as amplitude changes which represent meal-responses (**Fig. S1**). Four revised BSGM metrics have recently been developed to overcome several pitfalls of traditional EGG metrics (10), providing for accuracy improvements on top of the other advantages of BSGM over traditional EGG, including greater coverage over the stomach area to account anatomical variation of stomach location, a larger number of electrodes, modern bio-amplifiers, and validated signal processing techniques to decrease noise including signals from competing biological sources (3,7).

The revised BSGM metrics include BMI-Adjusted Amplitude, Principal Gastric Frequency, Gastric-Alimetry Stability Index (GA-RI), and Fed:Fasted Amplitude Ratio. Detailed descriptions of metrics are presented in **Supplementary Table 4**. Normative ranges for these revised BSGM spectral metrics were developed from a cohort of 110 health controls (11).

Patient phenotyping, as described in the methods, was subsequently completed by comparing individual subject-level data with these reference ranges.

SPATIAL ANALYSIS

The high-resolution electrode array was used to derive metrics to detect abnormal gastric slow wave activation patterns (12–15). The spatial metrics assessed in this study included ‘average spatial covariance’ and the percentage duration of retrograde wave propagation during the Gastric Alimetry test (3,7,14).

Average spatial covariance was defined by the average absolute value of the covariance between pairs of adjacent electrodes computed over the course of a Gastric Alimetry test.

Direction of slow wave propagation was determined by visually inspecting slow wave propagation animations averaged over 15 minute epochs per the methods of Gharibans et al (7). Example visualizations of phase map animations are displayed in **Figure S6.**

Strobe checklist

This study was reported according to the STROBE statement (16).

Supplementary Tables and Figures

Table S1: Medication and nicotine use

One participant with T1D did not withhold their domperidone on the study day. One participant with T1D was on pancreatic enzyme replacement taking Creon.

* Denotes at least once in the last 3 months but not in the last 48 hours prior to the study

Variable		Controls	T1D - no symptoms	T1D - symptoms	Total	p
Total N (%)		32 (50)	17 (27)	15 (23)	64	
Nicotine Use*	(%)	0 (0)	0 (0)	2 (13)	2 (3)	**0.034**
Cannabis use*	(%)	2 (6)	0 (0)	1 (7)	3 (5)	0.565
SLGT2 Inhibitor use	(%)	0 (0)	2 (12)	2 (13)	4 (6)	0.116
Metformin use	(%)	0 (0)	0 (0)	1 (7)	1 (2)	0.190
Prokinetic use	(%)	0 (0)	0 (0)	5 (33)	5 (8)	**<0.001**
Pain neuromodulator use	(%)	0 (0)	1 (6)	5 (33)	6 (9)	**0.001**
Opioid use	(%)	0 (0)	0 (0)	2 (13)	2 (3)	**0.034**
Selective serotonin reuptake inhibitor, benzodiazepine use	(%)	0 (0)	1 (6)	4 (27)	5 (8)	**0.006**
PPI use	(%)	3 (9)	4 (24)	6 (40)	13 (20)	**0.048**
Antiemetic use	(%)	0 (0)	0 (0)	2 (13)	2 (3)	**0.034**
Laxative use	(%)	0 (0)	0 (0)	1 (7)	1 (2)	0.190

Table S2: BSGM metrics, symptom, and quality of life data between controls and T1D patients with and without symptoms

P-values with Benjamini-Hochberg's corrections for multiple comparisons displayed. Sx, symptoms

Variable		Controls	T1D - no symptoms	T1D - symptoms	Total	p-value		
						T1D - no sx vs Controls	T1D – sx vs Controls	T1D - sx -T1D vs no sx
Total N (%)		32 (50)	17 (27)	15 (23)	64	-	-	-
BMI-adjusted amplitude (μV)	Median (IQR)	33.3 (27.1 to 50.0)	35.0 (33.0 to 40.9)	40.5 (25.7 to 47.8)	34.9 (27.1 to 50.0)	0.943	0.818	0.818
Fed:Fasted Amplitude Ratio	Median (IQR)	1.87 (1.47 to 2.22)	1.80 (1.36 to 2.26)	1.62 (1.51 to 2.13)	1.82 (1.42 to 2.25)	0.780	0.780	0.780
Principal Gastric Frequency (cpm)	Median (IQR)	3.09 (2.90 to 3.24)	3.06 (2.94 to 3.26)	3.35 (3.08 to 3.54)	3.12 (2.93 to 3.30)	0.491	0.237	0.347
Gastric Alimetry - Rhythm Index (GA-RI)	Median (IQR)	0.51 (0.39 to 0.75)	0.47 (0.32 to 0.57)	0.39 (0.26 to 0.51)	0.47 (0.34 to 0.61)	0.196	**0.017**	0.196
Principal Gastric Frequency Deviation	Median (IQR)	0.14 (0.10 to 0.25)	0.15 (0.06 to 0.28)	0.41 (0.13 to 0.54)	0.17 (0.09 to 0.32)	0.523	**0.048**	0.106
Average spatial covariance	Median (IQR)	0.51 (0.48 to 0.55)	0.49 (0.46 to 0.51)	0.48 (0.46 to 0.50)	0.50 (0.47 to 0.52)	0.058	**0.009**	0.353
Percentage time with retrograde wave propagation (%)	Median (IQR)	0.0 (0.0 to 12.1)	6.7 (0.0 to 30.6)	7.4 (0.0 to 19.6)	6.46 (0.00 to 16.67)	0.483	0.483	0.996
Mean fasting glucose (mmol/L)	Median (IQR)	NA	7.43 (6.10 to 10.07) *n = 17*	7.87 (7.82 to 10.65) *n = 3*	7.82 (6.55 to 10.07) *n = 20*	-	-	0.368
Mean post-meal glucose (mmol/L)	Median (IQR)	NA	9.33 (8.81 to 12.05) *n = 17*	8.85 (8.32 to 10.19) *n = 4*	9.31 (8.53 to 12.05) *n = 21*	-	-	0.654
Total Symptom Burden	Median (IQR)	0.01 (0.00 to 1.02)	0.34 (0.00 to 1.43)	11.73 (8.64 to 16.68)	0.44 (0.00 to 3.95)	0.346	**0.000**	**0.000**
GCSI	Median (IQR)	0.00 (0.00 to 0.22)	0.11 (0.00 to 0.44)	2.89 (1.39 to 3.44)	0.22 (0.00 to 0.89)	0.121	**0.000**	**0.000**
PAGI-SYM Score	Median (IQR)	0.10 (0.00 to 0.31)	0.15 (0.05 to 0.25)	2.35 (1.18 to 2.70)	0.22 (0.05 to 0.60)	0.556	**0.000**	**0.000**
PAGI-QoL Score	Median (IQR)	0.12 (0.00 to 0.32)	0.20 (0.03 to 0.43)	2.31 (1.26 to 3.43)	0.29 (0.06 to 0.53)	0.260	**0.000**	**0.000**

Variable		Controls	T1D - no symptoms	T1D - symptoms	Total	p-value		
						T1D - no sx vs Controls	T1D – sx vs Controls	T1D - sx -T1D vs no sx
STAI-SF Score	Median (IQR)	13.0 (10.0 to 15.5)	24.0 (22.0 to 29.0)	20.0 (16.5 to 31.0)	19.0 (12.5 to 24.0)	**0.000**	**0.007**	0.955
PHQ-2 Score	Median (IQR)	0.0 (0.0 to 0.5)	0.0 (0.0 to 1.0)	2.0 (1.0 to 3.5)	0.00 (0.00 to 1.00)	0.422	**0.002**	**0.003**

Table S3: Test quality

Variable		Controls	T1D - no symptoms	T1D - symptoms	Total	p-value		
						T1D - no symptoms vs Controls	T1D – symptoms vs Controls	T1D - symptoms- T1D vs no symptoms
Total N (%)		32 (50)	17 (27)	15 (23)	64	-	-	-
Impedance (kΩ)	Mean ± SD	107.9 ± 78.1	136.7 ± 66.7	186.6 ± 100.1	134.0 ± 85.8)	0.183	0.040	0.173
Marked artifact (% duration of study)	Mean ± SD	17.16 (11.75)	27.81 (19.41)	29.80 (16.68)	22.95 (16.13)	0.000	0.000	0.506
>50% meal completion	n (%)	32 (100)	17 (100)	14 (93)	63 (98)	0.234		

Table S4: BSGM metrics

Adapted from Schamberg et al. 2022 [10]

Metric	Description and rationale	Lower	Upper
BMI-Adjusted Amplitude (μV)	The amplitude/power (μV/dB) associated with dominant frequency in the overall spectrum is confounded by BMI. Gastric Alimetry therefore employs a conservative BMI-adjusted amplitude using a multiplicative regression.	20	70
Principal Gastric Frequency (cpm)	Dominant frequency calculations based on the highest average power across spectra are susceptible to transient bursts of low-frequency signal <2cpm, conflating non-gastric signals with gastric activity.[10] The 'principal gastric frequency' metric instead identifies only the frequency associated with the most stable oscillations, as measured by a distinct new stability metric (GA-RI; see below). The principal gastric frequency therefore detects the intrinsic gastric frequency, as opposed to simply calculating the frequency with the highest average power including all spectral contents whether gastric in origin or otherwise	2.65	3.35
Gastric Alimetry Rhythm Index (GA-RI)	Instability coefficient metrics vary in magnitude based on the dominant frequency (explained in further detail in Schamberg et al. 2022 [10]). The 'Gastric Alimetry Rhythm Index' (GA-RI), provides a measure of rhythmic gastric activity stability, by quantifying the extent to which activity is concentrated within a narrow frequency band over time relative to the residual spectrum. This improves on previous stability metrics in that it has no inherent dependence on the dominant frequency. As a result, the GA-RI enables independent assessment of the frequency and stability of gastric activity. Furthermore, the GA-RI includes a conservative BMI adjustment to account for the effect that signal attenuation has on the perceived relative strength of the gastric activity.	0.25	-
Fed:Fasted Amplitude Ratio	Amplitude increase following a meal stimulus is a characteristic of healthy gastric function. However, timing of the meal response varies. The Fed:Fasted Amplitude Ratio, instead quantifying the observed meal response by taking a ratio of the overall postprandial amplitude averaged over 4 hours to the preprandial amplitude, takes the ratio between the maximum amplitude in *any single 1-hour* across a 4-hour postprandial period to the amplitude in the preprandial period. Given that the goal of amplitude/power ratio metrics is to identify an increase in amplitude/power following meal consumption, it is important to have a metric that can quantify this increase across a cohort of subjects with significant natural variation in the timing of the meal response.	1.08	-

Figure S1: The Gastric Alimetry system

Adapted from Gharibans et al. [3]

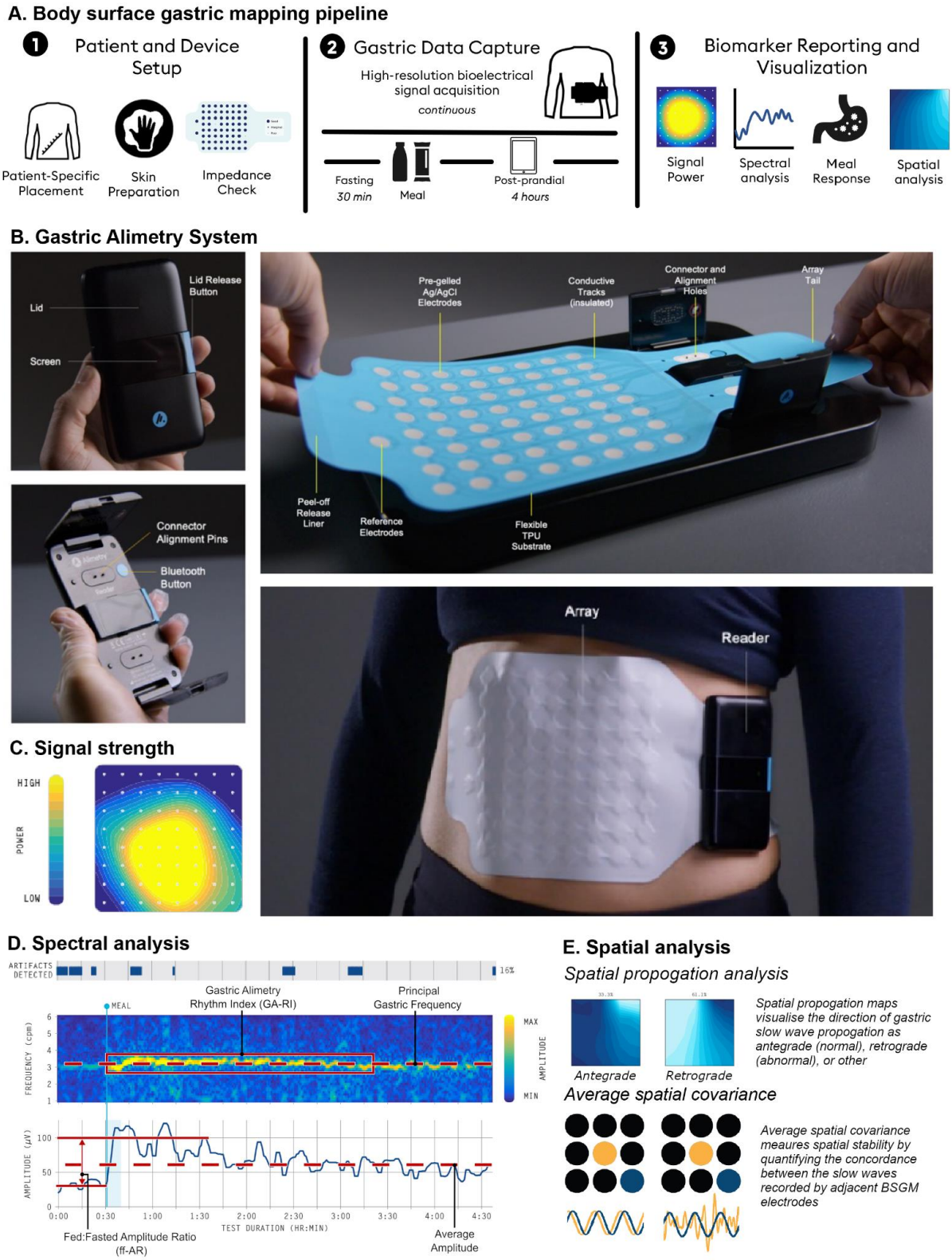

Figure S2:

Blood glucose levels (BGL) as measured by continuous glucose monitors during the study.

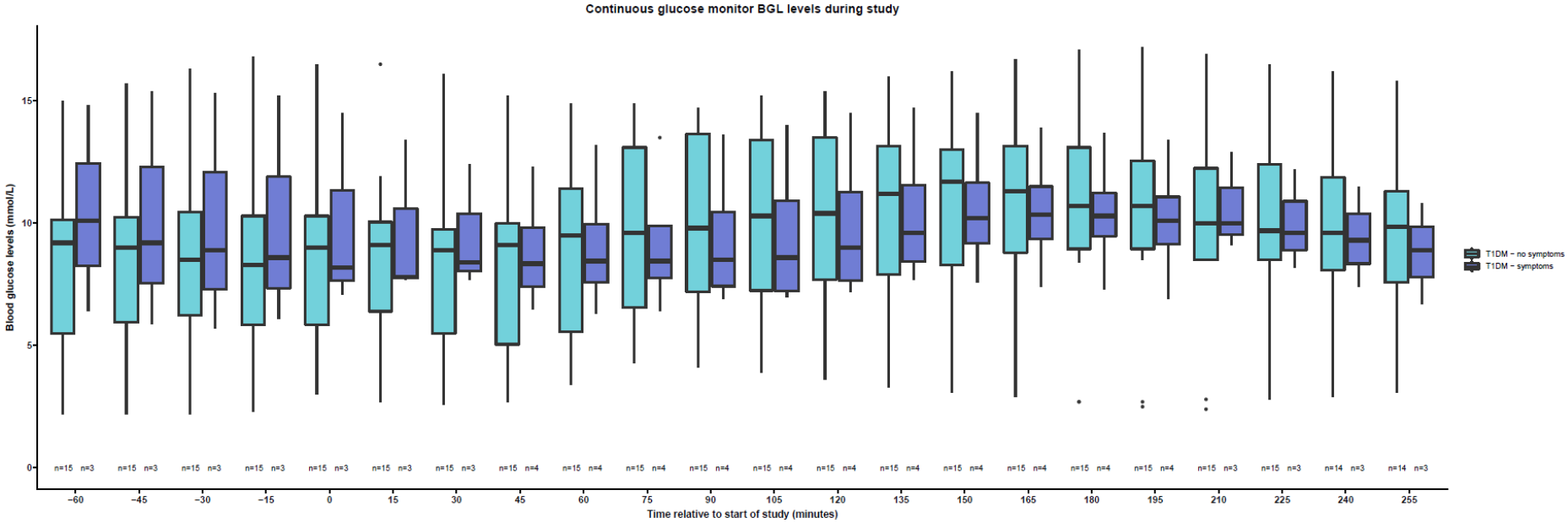

Figure S3:
Participant phenotype classification based on symptoms, spectrogram analysis and spatial propagation maps in this study. T1D, type 1 diabetes; sx, symptoms; CNVS, chronic nausea and vomiting syndrome; FD, functional dyspepsia; GA-RI, Gastric Alimetry Rhythm Index; PGF, principal gastric frequency; ffAR, Fed:Fasted Amplitude Ratio; SW, slow wave; BSGM, body surface gastric mapping.

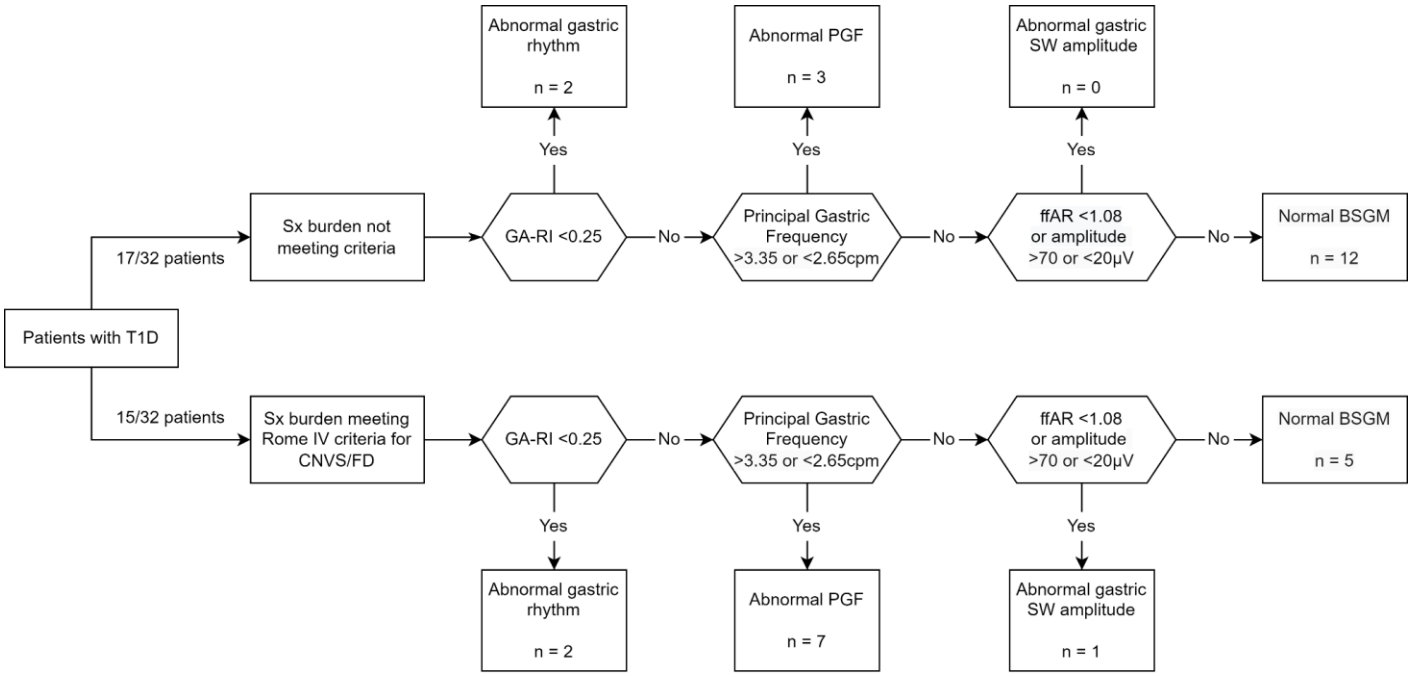

Figure S4: Association between Principal Gastric Frequency, amplitude and blood glucose levels

A) Within-individual pairwise Pearson R correlation coefficients for blood glucose versus amplitude averaged across phenotypes. Averaged across cohorts and compared across groups. Example plots of B) good within individual correlation between amplitude and BGL (r=0.736, p<0.001), C) poor correlation with a delayed BGL peak (r = 0.025, p=0.679), D) poor correlation with a high baseline BGL. BGL, blood glucose levels (r = -0.07, p =0.228).

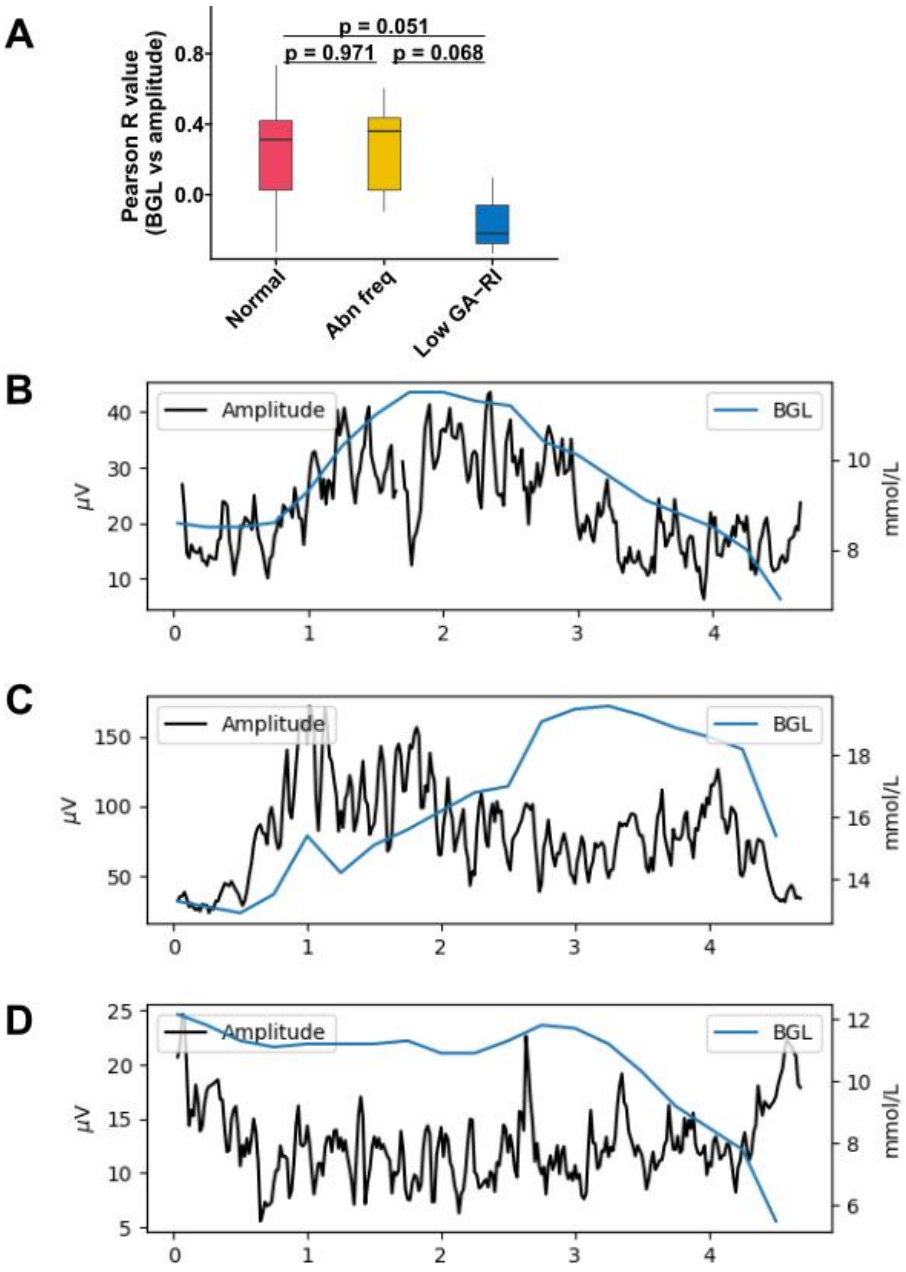

Figure S5: BSGM of T1D patient with abnormally high amplitude

Dark blue blocks within the spectrogram denote areas of high artifact. Note the adjusted amplitude scale relative to Figure 3.

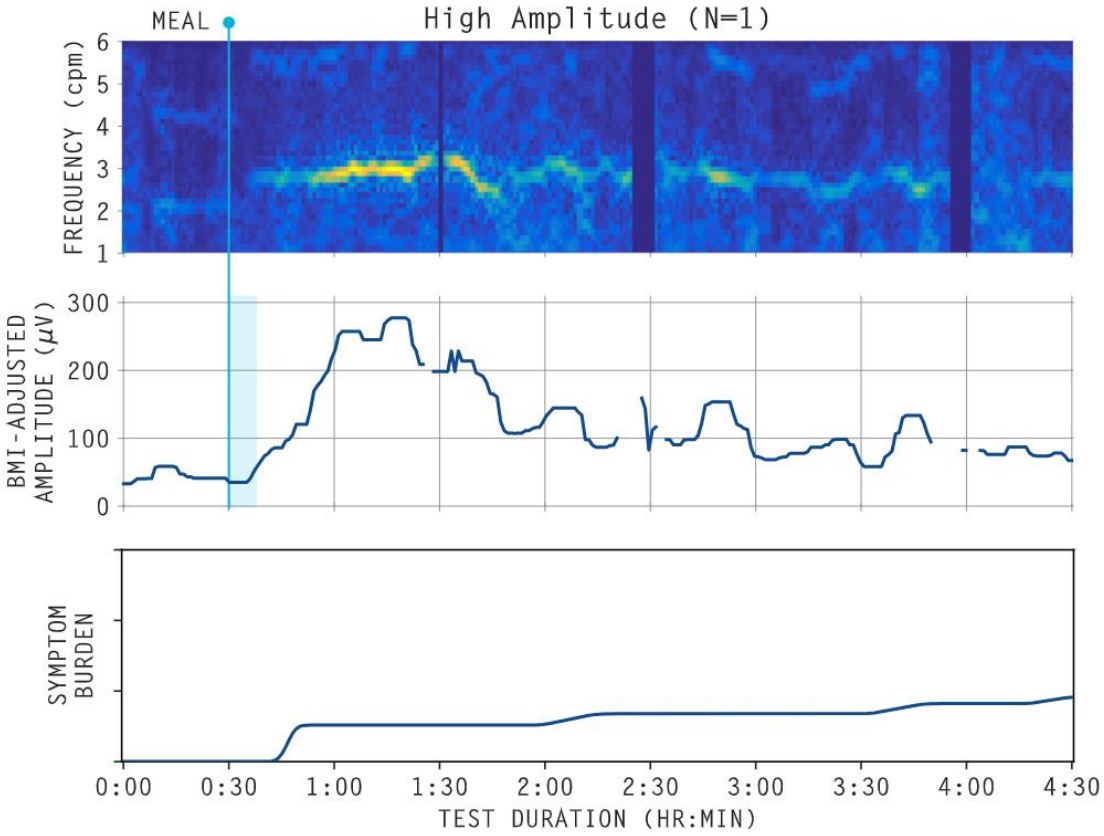

Figure S6: Antegrade and Retrograde Slow Wave Propagation

Spatial phase maps displaying the propagation of gastric slow waves averaged over 15 minute epochs. Frames 1 to 4 represent denote passage through time. Normal propagation is in the antegrade direction from the gastric fundus towards the gastric antrum and appears as right to left on the body surface (A).[12] Retrograde propagation in the opposite direction (B) is associated with pathological states and gastric symptoms.[14] When no clear antegrade or retrograde pattern was discernible from animations, the corresponding 15 minute epoch was marked as indeterminate.

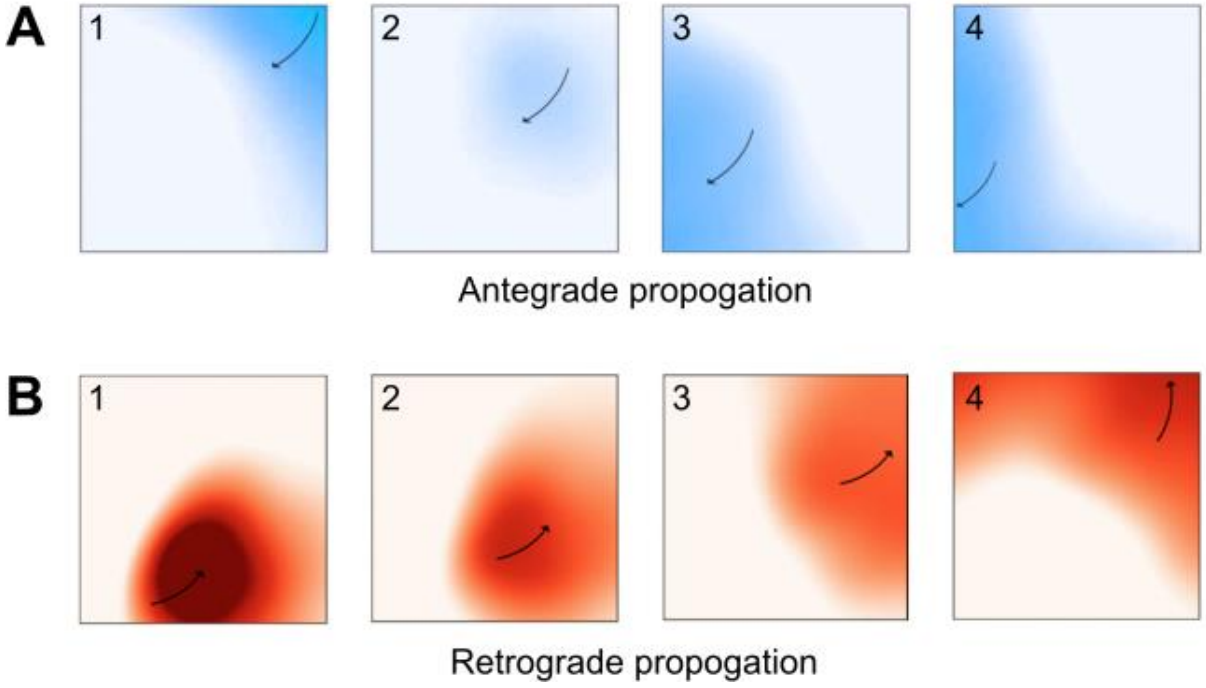

Supplementary references

1. Stevens PE, Levin A, Kidney Disease: Improving Global Outcomes Chronic Kidney Disease Guideline Development Work Group Members. KDIGO 2012 clinical practice guideline for the evaluation and management of chronic kidney disease. Kidney Int [Internet]. 2013; Available from: https://jhu.pure.elsevier.com/en/publications/kidney-disease-improving-global-outcomes-kdigo-ckd-work-group-kdi-4
2. Ricci Fabrizio, De Caterina Raffaele, Fedorowski Artur. Orthostatic Hypotension. J Am Coll Cardiol. 2015 Aug 18;66(7):848–60.
3. Gharibans AA, Calder S, Varghese C, Waite S, Schamberg G, Daker C, et al. Gastric dysfunction in patients with chronic nausea and vomiting syndromes defined by a novel non-invasive gastric mapping device. medRxiv. 2022 Feb 8;2022.02.07.22270514.
4. Gharibans, A. A. Coleman, T. Mousa, H. Kunkel, D. High-density multichannel electrode array improves the accuracy of cutaneous electrogastrography across subjects with wide-ranging BMI: 1235. Am J Gastroenterol [Internet]. 2018; Available from: https://journals.lww.com/ajg/fulltext/2018/10001/high_density_multichannel_electrode_array_improves.1235.aspx
5. Calder S, O'Grady G, Cheng LK, Du P. A Simulated Anatomically Accurate Investigation Into the Effects of Biodiversity on Electrogastrography. IEEE Trans Biomed Eng. 2020 Mar;67(3):868–75.
6. Angeli TR, Du P, Paskaranandavadivel N, Janssen PWM, Beyder A, Lentle RG, et al. The bioelectrical basis and validity of gastrointestinal extracellular slow wave recordings. J Physiol. 2013 Sep 15;591(18):4567–79.
7. Gharibans A, Hayes T, Carson D, Calder S, Varghese C, Du P, et al. A novel scalable electrode array and system for non-invasively assessing gastric function using flexible electronics. Neurogastroenterology & Motility. 2022 Jun 14;e14418.
8. Sebaratnam G, Karulkar N, Calder S, Woodhead JST, Keane C, Carson DA, et al. Standardized system and App for continuous patient symptom logging in gastroduodenal disorders: Design, implementation, and validation. Neurogastroenterol Motil. 2022 Feb 13;e14331.
9. Gharibans AA, Smarr BL, Kunkel DC, Kriegsfeld LJ, Mousa HM, Coleman TP. Artifact Rejection Methodology Enables Continuous, Noninvasive Measurement of Gastric Myoelectric Activity in Ambulatory Subjects. Sci Rep. 2018 Mar 22;8(1):5019.
10. Schamberg G, Varghese C, Calder S, Waite S, Erickson JC, O'Grady G, et al. Revised spectral metrics for body surface measurements of gastric electrophysiology [Internet]. bioRxiv. 2022. Available from: http://dx.doi.org/10.1101/2022.07.05.22277284
11. Varghese C, Schamberg G, Calder S, Waite S, Carson DA, Foong D, et al. Normative values for body surface gastric mapping evaluations of gastric motility using Gastric Alimetry: spectral analysis. medRxiv. 2022 Jul 26;2022.07.25.22278036.
12. O'Grady G, Angeli TR, Du P, Lahr C, Lammers WJEP, Windsor JA, et al. Abnormal initiation and conduction of slow-wave activity in gastroparesis, defined by high-resolution electrical mapping. Gastroenterology. 2012 Sep;143(3):589–98.e3.

13. Angeli TR, Cheng LK, Du P, Wang THH, Bernard CE, Vannucchi MG, et al. Loss of Interstitial Cells of Cajal and Patterns of Gastric Dysrhythmia in Patients With Chronic Unexplained Nausea and Vomiting. Gastroenterology. 2015 Jul;149(1):56–66.e5.
14. Gharibans AA, Coleman TP, Mousa H, Kunkel DC. Spatial Patterns From High-Resolution Electrogastrography Correlate With Severity of Symptoms in Patients With Functional Dyspepsia and Gastroparesis. Clin Gastroenterol Hepatol. 2019 Dec;17(13):2668–77.
15. Somarajan S, Muszynski ND, Olson JD, Comstock A, Russell AC, Walker LS, et al. The effect of chronic nausea on gastric slow wave spatiotemporal dynamics in children. Neurogastroenterol Motil. 2021 May;33(5):e14035.
16. von Elm E, Altman DG, Egger M, Pocock SJ, Gøtzsche PC, Vandenbroucke JP, et al. The Strengthening the Reporting of Observational Studies in Epidemiology (STROBE) statement: guidelines for reporting observational studies. Ann Intern Med. 2007 Oct 16;147(8):573–7.